Geophysical Research Letters®

All the authors are listed in alphabetical order except "Zhiyi Jiang and Chris M. Brierley."

Key Points:

- A multi-model ensemble of Holocene transient simulations by general circulation models has been assembled
- Although some models show changes, no consistent trend in overall Atlantic Meridional Overturning Circulation (AMOC) strength during the mid-to-late Holocene emerges from the ensemble
- We interpret this result to suggest no overall change in AMOC, which fits with our assessment of available proxy reconstructions

Supporting Information:

Supporting Information may be found in the online version of this article.

Correspondence to:

Z. Jiang,
z.jiang.17@ucl.ac.uk

No Consistent Simulated Trends in the Atlantic Meridional Overturning Circulation for the Past 6,000 Years

Zhiyi Jiang[1] [ID], **Chris M. Brierley[1]** [ID], **Jürgen Bader[2]** [ID], **Pascale Braconnot[3]** [ID], **Michael Erb[4]** [ID], **Peter O. Hopcroft[5]** [ID], **Dabang Jiang[6]** [ID], **Johann Jungclaus[2]** [ID], **Vyacheslav Khon[7,8]** [ID], **Gerrit Lohmann[9]** [ID], **Olivier Marti[3]**, **Matthew B. Osman[10,11]** [ID], **Bette Otto-Bliesner[12]** [ID], **Birgit Schneider[13]** [ID], **Xiaoxu Shi[9]** [ID], **David J. R. Thornalley[1]** [ID], **Zhiping Tian[6]** [ID], and **Qiong Zhang[14,15]** [ID]

[1]Department of Geography, University College London, London, UK, [2]Max-Planck-Institut für Meteorologie, Hamburg, Germany, [3]Laboratoire des Sciences du Climat et de l'Environnement-IPSL, Gif-sur-Yvette, France, [4]School of Earth and Sustainability, Northern Arizona University, Flagstaff, AZ, USA, [5]School of Geography, Earth and Environmental Sciences, University of Birmingham, Birmingham, UK, [6]Institute of Atmospheric Physics, Chinese Academy of Sciences, Beijing, China, [7]Lyell Centre, Heriot-Watt University, Edinburgh, UK, [8]A. M. Obukhov Institute of Atmospheric Physics, Russian Academy of Sciences, Moscow, Russia, [9]Alfred-Wegener-Institut Helmholtz-Zentrum für Polar-und Meeresforschung, Bremerhaven, Germany, [10]Department of Geography, University of Cambridge, Cambridge, UK, [11]Department of Geosciences, University of Arizona, Tucson, AZ, USA, [12]National Center for Atmospheric Research (NCAR), Boulder, CO, USA, [13]Institute of Geosciences, Kiel University, Kiel, Germany, [14]Department of Physical Geography, Stockholm University, Stockholm, Sweden, [15]Bolin Centre for Climate Research, Stockholm University, Stockholm, Sweden

Abstract The Atlantic Meridional Overturning Circulation (AMOC) is a key feature of the North Atlantic with global ocean impacts. The AMOC's response to past changes in forcings during the Holocene provides important context for the coming centuries. Here, we investigate AMOC trends using an emerging set of transient simulations using multiple global climate models for the past 6,000 years. Although some models show changes, no consistent trend in overall AMOC strength during the mid-to-late Holocene emerges from the ensemble. We interpret this result to suggest no overall change in AMOC, which fits with our assessment of available proxy reconstructions. The decadal variability of the AMOC does not change in ensemble during the mid- and late-Holocene. There are interesting AMOC changes seen in the early Holocene, but their nature depends a lot on which inputs are used to drive the experiment.

Plain Language Summary The Atlantic Meridional Overturning Circulation (AMOC) is a deep ocean circulation system that is both important for climate and vulnerable to climate changes. Here we use a set of multiple climate models to look at how the AMOC responded to changes in climate drivers over the past few thousand years. The changes are only small in all of the models, and do not agree in their direction. The AMOC naturally varies on decadal timescales, but we do not see any strong trends in its variability either. We consider these simulations to indicate that the overall AMOC has not changed over the past 6,000 years, which fits with recent data reconstructions.

1. Introduction

The Atlantic Meridional Overturning Circulation (AMOC, Rahmstorf, 2006) is a large-scale ocean circulation that helps transport heat poleward moderating the climate of Europe and eastern North America (Cherchi, 2019). Direct observations of it only became available in 21st century, and show a noticeable weakening (Smeed et al., 2018) that is not captured in full by climate models (Weijer et al., 2020), potentially because it arises from natural variability. Despite this, the IPCC Assessment Report 6 projects a further weakening in AMOC strength with high confidence (Fox-Kemper et al., 2021), although the magnitude remains uncertain. Evaluating the response of models to past variations in boundary conditions (such as orbital configuration and greenhouse gases levels, ice sheet extent) against proxy-derived reconstructions of the AMOC can potentially help constrain the uncertainty in future projections (Kageyama et al., 2018).

The Holocene Epoch (roughly the past 12,000 years) saw gradual changes in the seasonal cycle of incoming solar radiation caused by changes in the orbital configuration (Braconnot et al., 2019; Otto-Bliesner et al., 2017). There were also decreasing greenhouse gases (GHG; CO_2, CH_4, and N_2O) concentrations, followed by an increase that

is gradual until industrialization and very rapid afterward (He, 2011; Tian et al., 2022). The decaying ice-sheets released meltwater throughout the early Holocene (Argus et al., 2014; Peltier et al., 2015), with an abrupt release into the Labrador Sea during the 8.2 ka event (Aguiar et al., 2021). Reconstructions also show variations in anthropogenic land-use, total solar irradiance (Vieira et al., 2011), and volcanic activity (Kobashi et al., 2017) that was particularly strong at 8.6–8 and 7.5–7 ka BP.

A large amount of different proxies have been used to reconstruct AMOC during the Holocene. These have been assessed to show a relatively stable overall AMOC strength (excepting several abrupt events) until a weakening during the Industrial period (Gulev et al., 2021). It can often be unclear whether individual reconstructions are tracking the integrated flow throughout overturning circulation or just a particular, local component. Reconstructions from both vertical density gradient (Lynch-Stieglitz et al., 2009) or based on Pa/Th ratios (e.g., Hoffmann et al., 2018; Lippold et al., 2019; Ng et al., 2018) suggest little change in the overall AMOC strength since 9,000 years ago. Data assimilation approaches similarly suggest little long-term AMOC change in the Holocene (Osman et al., 2021; Ritz et al., 2013). Higher temporal resolution reconstructions for the past 2,000 years also show little change in overall AMOC, but exhibit uncertainty about the timing and nature of the Industrial Era decline (Caesar et al., 2021; Thornalley et al., 2018; Valley et al., 2022). Reconstructions exist that propose different temporal behavior; combining all the existing records to provide a complete picture of all aspects of the AMOC remains an ongoing effort.

Snapshot equilibrium simulations for 6,000 years ago (6 ka) have been performed for the *midHolocene* experiment of the Palaeoclimate Modeling Intercomparsion Project (PMIP, Kageyama et al., 2018). Brierley et al. (2020) found that the AMOC strength in the *midHolocene* ensemble is not markedly different. These results are supported by associated simulations of the last interglacial (Jiang et al., 2023). There is known to be a resolution dependency (Shi & Lohmann, 2016; Shi et al., 2020), which itself could vary by model (Jackson et al., 2020).

Currently there is an effort in the community to undertake transient Holocene simulations, which focus on analyzing the time-dependent interactions between different components in the Earth system and the long-term climate evolution. Here we collate the emerging set of Holocene transient simulations from different modeling groups to further investigate whether there is a consistent message from the ensemble about trends in (a) AMOC strength, (b) its spatial structure, and (c) its internal decadal variability since 6,000 years ago. Summary information about the different transient simulations is given in Section 2, along with an explanation of the analysis procedures. Further information about each of the individual simulations can be found in Supporting Information S1. The results of the AMOC trends in Holocene transient runs are presented in Section 3, followed by discussion and conclusions in the last section.

2. Data and Methods

We use nine transient model simulations from eight different coupled climate models (summarized in Table 1). All of the simulations are run continuously toward the present day from 6 ka or earlier. Not all of the models are truly independent: EC-Earth3-veg-LR, KCM, and IPSL-CM5 use NEMO ocean model at different resolutions (Crosta et al., 2018; Madec et al., 2008); AWI-ESM-2, MPI-ESM, and KCM have versions of the ECHAM atmosphere (Mauritsen et al., 2019; Roeckner et al., 2003; Shi et al., 2020; Sidorenko et al., 2019).

All simulations incorporate changes in the orbital configuration, and their associated changes in the seasonal distribution of incoming solar radiation across Earth (Otto-Bliesner et al., 2017). Also varying concentrations of well-mixed greenhouse gases are specified in every simulation using ice-core records, although the precise reconstructions used do differ. Those simulations that start in the early Holocene generally incorporate changes in ice-sheet topography and their associated changes in the land-sea mask (Hopcroft & Valdes, 2021; Otto-Bliesner et al., 2006; Tian et al., 2022). Only the simulations with CCSM3 impose meltwater fluxes implied by changes in ice-sheet topography. Reconstructions of volcanic forcing and variations in total solar irradiance introduce forced variability into the simulations, although this has only been done in a single simulation (Dallmeyer et al., 2021). Anthropogenic impacts on global vegetation started with the development of farming in the early Holocene, but became much more substantial approaching the industrial period (Smith & Zeder, 2013). These are incorporated by MPI-ESM using the reconstructions after Hurtt et al. (2011) and Lawrence et al. (2016), but only for the last millennium (850–1850 CE).

The zonal-averaged meridional overturning streamfunction in the Atlantic basin is computed for each decade. Given that the data are decadally averaged, calendar adjustments to account for variations in the month lengths

Table 1
The Ensemble of Holocene Transient Simulations, Their Experimental Design and Primary Publication About the Individual Model Description

Model	Length of run (ka BP)	Forcings	Ocean resolution (horizontal, vertical)	Reference
AWI-ESM-2	6–0	Orbital, GHG	Multi-resolution (finest 25 km in polar), 46 levels	Shi et al. (2022)
IPSL-CM5[a]	6–0	Orbital, GHG	Longitude 2°, latitude 0.5–2° (finer near equator), 31 levels	Braconnot et al. (2019)
MPI-ESM[b]	7.95–0.1	Orbital, GHG, land-use, ozone, with or without volcanic and solar	1.5° Horizontal grid, 41 levels	Bader et al. (2020)
EC-Earth3-veg-LR	8–0	Orbital, GHG	1° Horizontal grid, 75 levels	Zhang et al. (2021)
HadCM3-M2.1d[c]	10–0	Orbital, GHG, ice-sheets and sea-level	1.25° × 1.25°, 20 levels	Hopcroft and Valdes (2021)
KCM	9.5–0	Orbital, GHG	Longitude 2°, latitude 0.5–2° (finer near equator), 31 levels	Segschneider et al. (2018)
CCSM3	22–0	Orbital, GHG, land-ice, meltwater	Longitude 3.6°, latitude varies (finer 0.9° near equator), 25 levels	Otto-Bliesner et al. (2006)
CESM1.2.1	11.5–0.1	Orbital, GHG, ice-sheets and topography	1° Horizontal grid, 60 levels	Tian et al. (2022)

[a]This simulation is referred to as "TR5AS-Vlr01" in Braconnot et al. (2019). [b]Two simulations of MPI-ESM are used here: SLO50 is the main focus of Bader et al. (2020) and includes volcanic and solar forcing variations, SLO43 does not include them and is only considered as a sensitivity run in Bader et al. (2020). [c]In this study, we use the simplest of the HadCM3-M2.1d ensemble members, which is the "xokm" simulation.

(Shi et al., 2022) should not matter. Therefore, they have not been applied. The strength of the AMOC is taken as the maximum streamfunction at 30°N below 500 m after Brierley et al. (2020). The computation of the standard deviation of the AMOC at 30°N below 500 m is based on a sliding 100-year time window, starting from at earliest 7 ka BP.

3. Results

3.1. Trends in Maximum AMOC Strength

The evolution of maximum AMOC strength in each transient simulation is shown in Figure 1. Changes in AMOC since industrialization are not captured through a combination of the varying simulation end dates and the 100-year running mean used to smooth the time series. Absolute AMOC strength differs substantially between the models (Figure 1), which is mainly due to the model physics. Two simulations—AWI-ESM-2 (Shi et al., 2022) and CCSM3 (Otto-Bliesner et al., 2006)—show an overall increasing trend throughout their simulation years, but they differ in timing: AWI-ESM-2 sees an enhancement of the AMOC by 10% during 6–4 ka BP, after which the AMOC remains relatively stable and a slight decreasing trend is shown in the late Holocene. The increasing trend in CCSM3 is dominated by the strengthening of AMOC in the early to mid-Holocene, with only a subtle trend from 6 ka BP onwards. Conversely three simulations show an overall decreasing AMOC trend for the maximum AMOC: IPSL-CM5 (~2 Sv), EC-Earth3-veg-LR (~1 Sv) and KCM. In KCM there is a decrease of approximately 10% in the early portion, but after roughly 6 ka it remains relatively stable with a marginal increase in the late Holocene (Segschneider et al., 2018). The other simulations do not show any obvious trends in the overall maximum AMOC strength at 30°N through the Holocene (MPI-ESM, HadCM3 and CESM1.2.1). Both transient runs with the MPI-ESM (SLO0043 and SLO0050) do display a slightly higher maximum AMOC strength at 8 to 6 ka BP compared to later periods in the Holocene. In HadCM3, the AMOC strength before and after the 8.2 ka event remain relatively stable at ~19.5–21 Sv. CESM1.2.1 exhibits a step-change at 7.5 ka BP, but the AMOC is very stable afterward.

All the simulations that start in the early Holocene (CCSM3, HadCM3, KCM, and CESM1.2.1) show stronger changes in AMOC prior to 8 ka than afterward. The early Holocene saw the 8.2 ka event with a large amount of meltwater entering into the Labrador Sea (e.g., Barber et al., 1999; Matero et al., 2017) through three possible freshwater sources: the sudden discharge of Lake Agassiz, the altered route of the continental freshwater in the North America due to the Laurentide ice sheet melting, and the continuous retreat of Laurentide ice sheet and meltwater release from 9 to 6 ka BP (Aguiar et al., 2021). However, the different forcings imposed in the simulations (Table 1) mean that only CCSM3 responds directly to a changed meltwater flux.
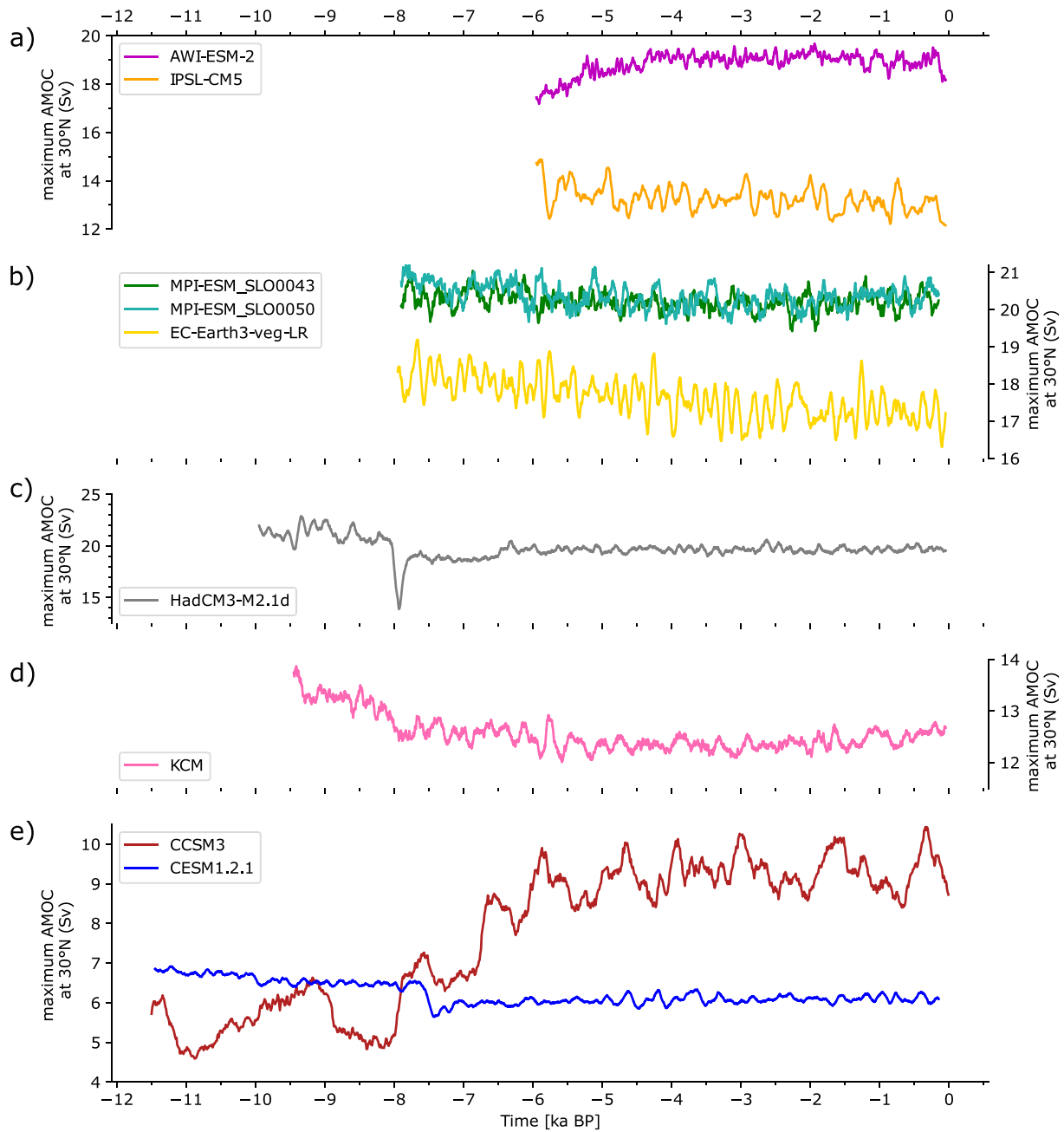
Figure 1. Evolution of the Atlantic Meridional Overturning Circulation (AMOC) in nine climate model simulations. The AMOC strength is tracked by the maximum meridional overturning streamfunction at 30°N below 500 m (at a decadal resolution, smoothed by a 100-year running mean). Note the different vertical scales.

The early Holocene decline in KCM arises primarily from model drift (Segschneider et al., 2018), but may include an AMOC response to increasing Greenhouse gases (as the lack of a continued trend into the late Holocene rules out an orbital influence). The sudden reduction in AMOC strength in HadCM3 around 8 ka BP arises from the opening of Hudson Bay, when the land sea mask is updated. This connected a large volume of freshwater to the Atlantic and weakened the AMOC for around 250 years. The run with CESM1.2.1 demonstrates an abrupt decrease in AMOC strength by 18% at 7.7–7.5 ka BP, after which the AMOC recovered and stabilized, but never returned to the same intensity as that in the early Holocene. The accumulated effect of the rapid retreat of the

Laurentide ice sheet from 9 to 7 ka BP (Tian et al., 2022) could be the main cause for the abrupt weakening of AMOC at around 7.7 ka BP in this run.

In conclusion, the transient simulations do not show any AMOC changes over the past 6,000 years that are "consistent" (i.e., with a majority of models showing statistically significant changes in the same direction). They do not have a consistent message about the small changes in the overall AMOC strength, as they show trends in different directions (Table S1 in Supporting Information S1) that are roughly three orders of magnitude less than those projected over the coming century (Fox-Kemper et al., 2021; Weijer et al., 2020). Several models simulate changes of roughly ±10%, but these are not of the same sign across models, nor do they exhibit similar temporal behaviors. The few simulations that start in the early Holocene all exhibit stronger changes prior to 6 ka BP than afterward. This is likely related to the loss of the remnant glacial ice through either meltwater or sea-level changes.

3.2. Trends in Spatial Structure of Streamfunction

There could be robust changes in the spatial structure of the AMOC, even if the ensemble members show little change in its overall strength. We investigate this possibility by mapping the trend in overturning streamfunction at each grid box from 6 ka BP to present (Figure 2). Different forms of AMOC evolution emerge—some models show the whole circulation spinning up (or down) together, whilst others demonstrate more complex structure (such as a subsurface warming at 30°N with cooling on either side of it).

Four simulations show broadly coherent changes in streamfunction especially visible in the deep southward return flow at 30°–50°N, 1,700–3,000 m (Figures 2b, 2e, and 2g show coherent decreasing trends; Figure 2h shows coherent increasing trends). IPSL-CM5, EC-Earth3-veg-LR, and KCM show an opposite direction of trend compared to CCSM3, as might be expected given their opposite trends in maximum AMOC strength (Figure 1). A tripole pattern in the mid-latitudes, extending down to ~1,200 m, is seen in the simulations by MPI-ESM, HadCM3 (Figures 2c, 2d, and 2f). Variations in the Mediterranean outflow could potentially be one of the causes lead to this pattern, given the latitude. Ivanovic et al. (2013) explore the impact of the Mediterranean outflow parameterization in one of the models used here, HadCM3, and demonstrate that it can create changes in AMOC of a similar spatial pattern (Ivanovic et al., 2014). Swingedouw et al. (2019) show the pattern of Mediterranean outflow changes are model dependent though. AWI-ESM-2 (Figure 2a) shows a pattern that combines both this upper-ocean mid-latitude tripole and a broad shift below 1,700 m. The CESM1.2.1 transient run has the weakest trend among all the simulations (Figure 2i), with almost no trend at any individual sites for the North Atlantic basin from 6 to 0.1 ka BP.

Taken as an ensemble, the simulations do not demonstrate a consistent trend in meridional streamfunction from 6 to 0 ka BP at any individual locations. Rather they highlight a range of possible behavior—from coherent changes throughout the basin or more nuanced patterns showing both strengthening and weakening at different locations.

3.3. Trends in AMOC Variability

The key difference between the two MPI-ESM simulations is the inclusion of externally forced variability (Bader et al., 2020). This motivates us to explore the AMOC variability throughout the Holocene, which we assess using the standard deviation of the decadally averaged, maximum overturning streamfunction at 30°N calculated over a sliding 100-year time window (Figure 3). However, there is clearly a strong role for internal variability in AMOC, as MPI-ESM SLO0050 shows roughly the same standard deviations as SLO0043 despite the addition of volcanic and solar forcing.

The magnitude of the (internal) variability varies substantially between simulations (Figure 3). The run with CESM1.2.1 has the smallest magnitude of the internal variability and indicates its simulated AMOC is very stable since 7 ka BP. Meanwhile, the transient runs with CCSM3, IPSL and KCM model also demonstrate relatively smaller magnitude compared to all other runs. Other simulations typically show a magnitude of the internal variability ranging from 1 to 1.5 Sv, with the strongest fluctuations in AWI-ESM2, IPSL, and EC-Earth3-veg-LR.
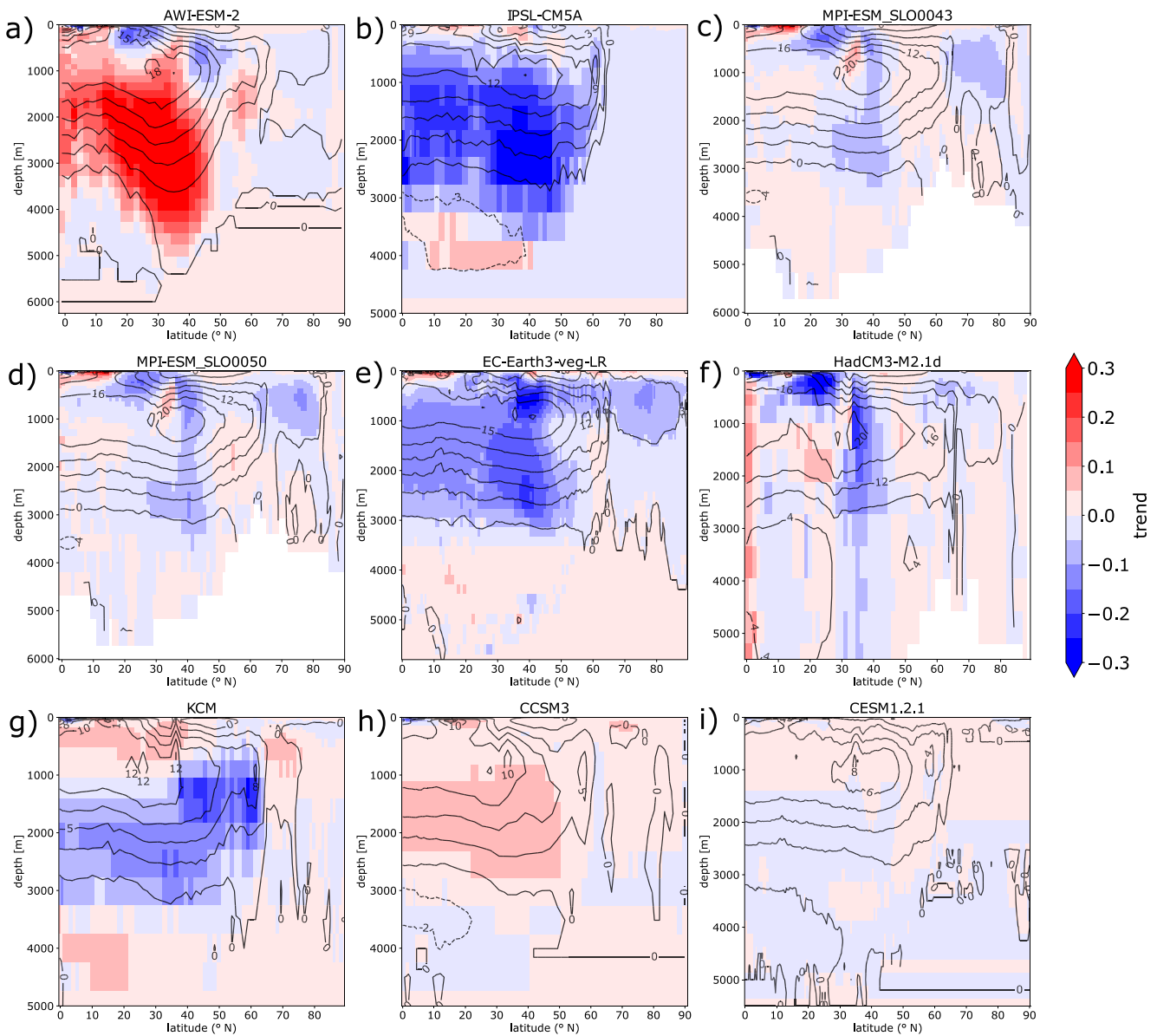
Figure 2. Trend in the meridional streamfunction in the North Atlantic Ocean from 6 ka BP to present (Sv/kyr). The overlaid contours are the mean Atlantic Meridional Overturning Circulation spatial pattern at 6–0 ka BP in each model: (a) AWI-ESM-2, (b) IPSL-CM5A, (c) MPI-ESM_SLO0043, (d) MPI-ESM_SLO0050, (e) EC-Earth3-veg-LR, (f) HadCM3-M2.1d, (g) KCM, (h) CCSM3, and (i) CESM1.2.1.

The CCSM3 simulation also demonstrates a millennium internal variability for the maximum AMOC at 30°N in the Holocene—this not seen in any other model (Figure 1), nor in other simulations with the same model (He & Clark, 2022).

None of the simulations show a large trend in the standard deviations (Figure 3). Over the past 6,000 years, only CCSM3 shows a small trend that is statistically significant (Table S1 in Supporting Information S1), and even that becomes insignificant if the analysis is extended back to 7 ka. Therefore, the ensemble as a whole shows no trend in the decadal variability of the maximum AMOC at 30°N (Figure 3; similarly for multi-decadal variability, Figure S2 in Supporting Information S1). We conclude that the internal variability of the AMOC remained constant during mid- and late Holocene, at least in models.
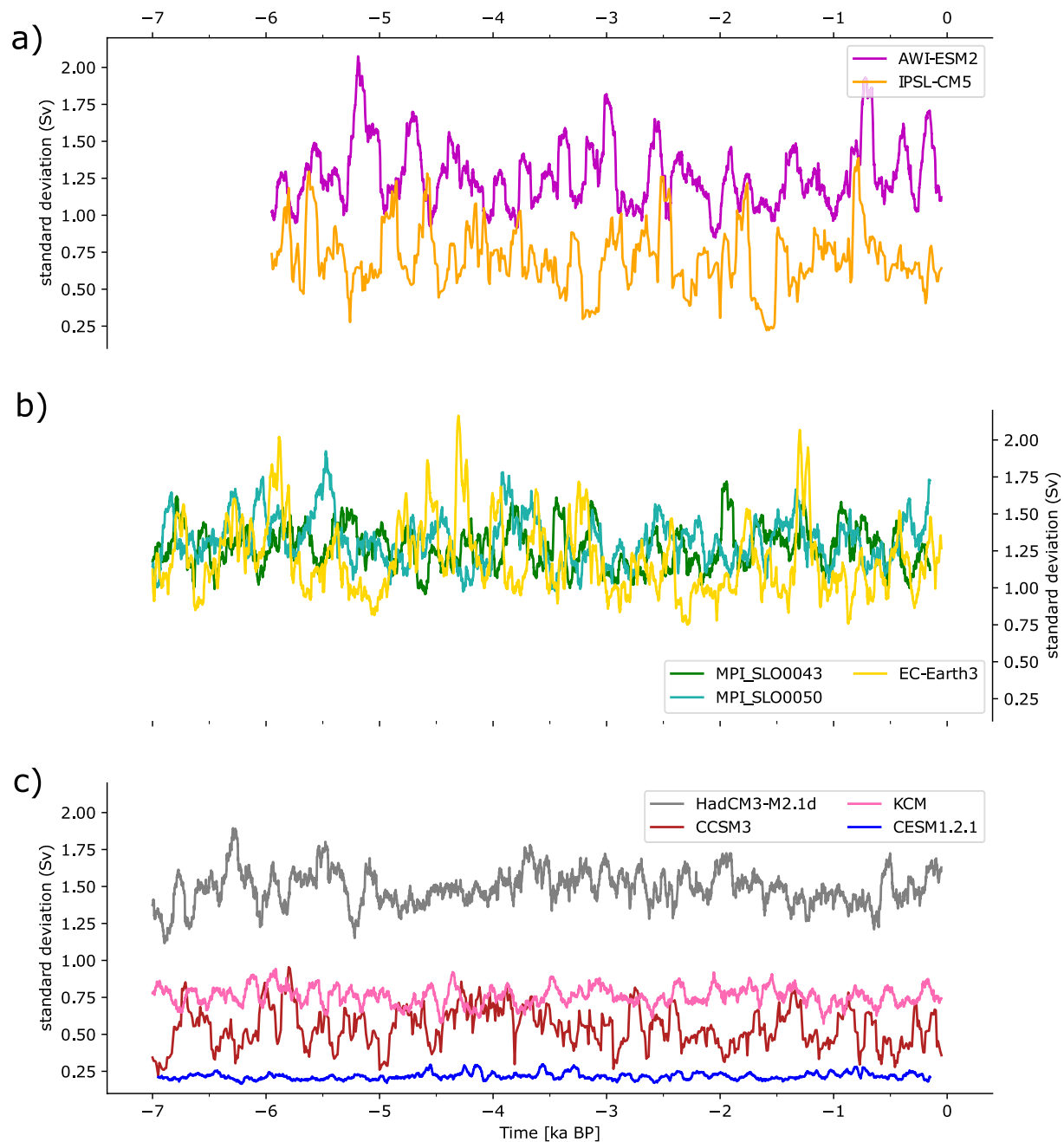
Figure 3. Running standard deviations of the maximum Atlantic Meridional Overturning Circulation strength at 30°N below 500 m from 7 ka BP to present (based on a sliding 100-year time window).

4. Discussion and Conclusions

Overall, there is little support from this ensemble of simulations for major changes in AMOC over the past 6,000 years. This is true for long-term trends in overall AMOC strength: although individual models may show small trends, there is no consistency in the direction of their changes. It is also true for internal variability of the AMOC. The different experimental set-ups used in the simulations did not appear to play a large role in AMOC evolution since 6,000 years ago, but there were clear consequences from the choice of imposed forcings in the early Holocene. This conclusion fits well with results from PMIP, which performed snapshot simulations for
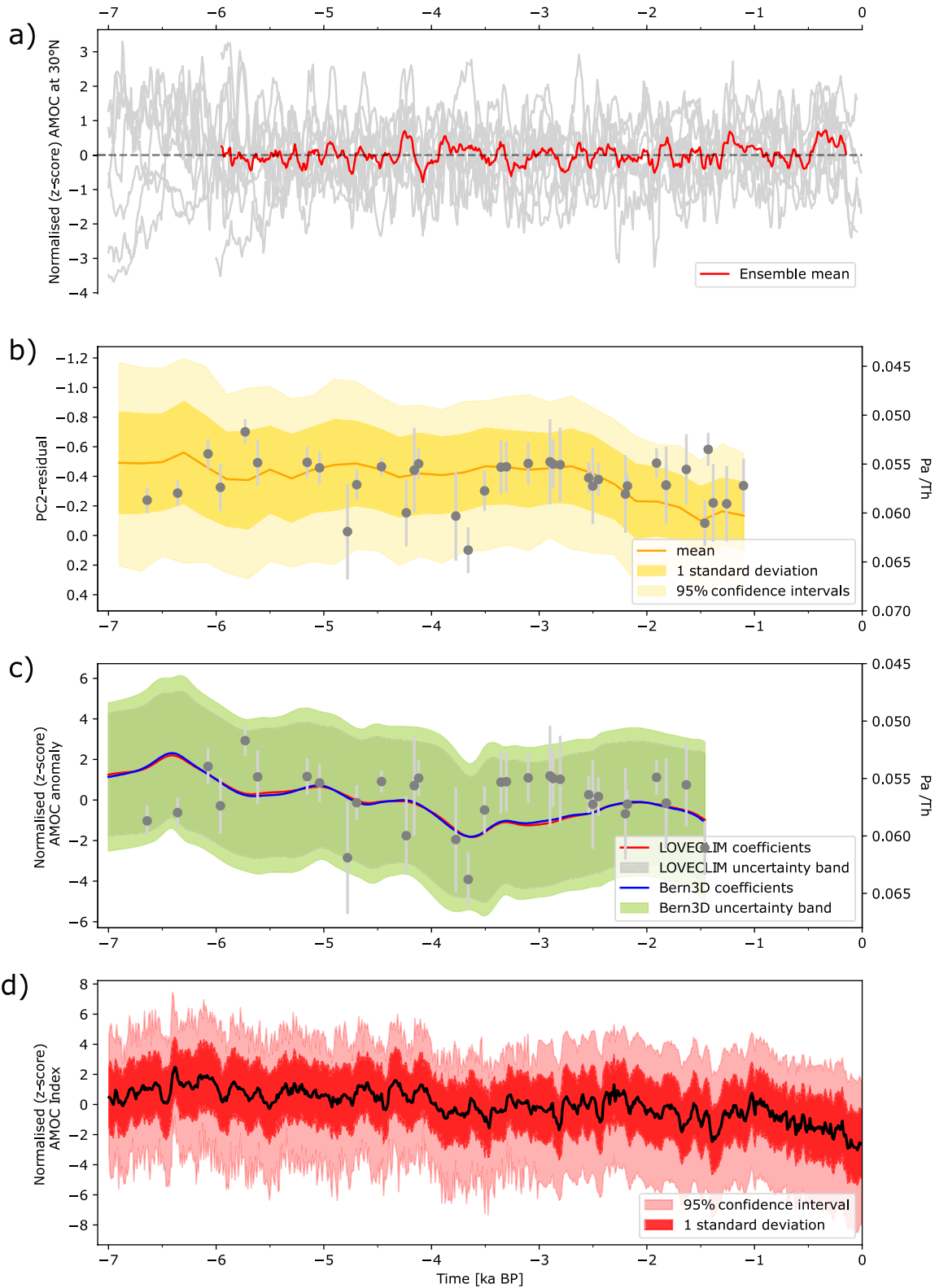
Figure 4.

6,000 years ago. They also found no consistent changes in AMOC strength (Brierley et al., 2020). Combining those mid-Holocene snapshot simulations alongside last interglacial simulations suggests that variations in precession would not be expected to alter AMOC (Jiang et al., 2023).

Our interpretation of the ensemble of Holocene transient model simulations as indicating no changes in AMOC agrees with various reconstructions of the overall AMOC (Figure 4). These include Pa/Th reconstructions, which have the benefit of (at least potentially) recording the integrated strength of AMOC from a few key sites (Lippold et al., 2019). Multiple independent AMOC reconstructions based upon data assimilation are also now available (Osman et al., 2021; Ritz et al., 2013). Additionally, the winter SST index of Caesar et al. (2018) can be applied to Holocene reconstructions of temperature anomalies (in this instance from Erb et al., 2022) to reconstruct past Holocene AMOC strength. Because this reconstruction represents annual mean temperature instead of November–May SST, the correlation to AMOC is likely slightly weakened and a direct conversion to absolute AMOC changes is not appropriate. Nonetheless this SST fingerprint approach should retain the timing and directions of any AMOC deviations and trends. Collectively these reconstructions also show little change in the AMOC during the mid-to-late Holocene (Figure 4).

Although the IPCC assessment of reconstructions suggest little change in AMOC during most of the past 6,000 years (Gulev et al., 2021), there are several proxy reconstructions that posit a late Holocene decline (Ayache et al., 2018; Valley et al., 2022). It may be that these reflect changes in individual components of the AMOC, such as Iceland-Scotland overflow water. Prior research suggests that strengthened deep water formation in the Labrador Sea could be compensated for by decreased deep water formation in the Nordic Seas, resulting in no change in overall AMOC (Renssen et al., 2005). All the data assimilation efforts (Figures 4b–4d) seem to show AMOC tail off toward the end of their respective records. These drops are not captured by the transient simulations, nor do proxy reconstructions show a strong long-term decrease over the last 2,000 years (Figure S1 in Supporting Information S1, Rahmstorf et al., 2015; Thornalley et al., 2018). Further work combining simulations and proxy reconstructions to explore possible compensation between different sub-components of the AMOC may provide useful additional information on future AMOC projections.

It has been suggested that the AMOC may play a role in Holocene centennial events, such as the 4.2 ka and 2.8 ka BP events (e.g., Denton & Broecker, 2008; Jalali et al., 2019; Keigwin & Boyle, 2000; Oppo et al., 2003). None of the individual transient simulations capture an event around 4.2 or 2.8 ka (Figure 1), nor do the assimilation products (Figure 4, although it is questionable whether they have sufficient temporal resolution to detect them). Nonetheless the weakest two centennial-scale periods of ensemble mean AMOC occur at ~4.2 and 2.8 ka (Figure 4a), which warrants further investigation. This is especially intriguing as explanations involving volcanic or solar forcing seem unlikely as the majority of simulations do not include these forcings.

In summary, this research implies that the overall AMOC maintained its strength over the past 6,000 years until the recent changes. The evidence for this conclusion comes from an ensemble of transient simulations using fully coupled general circulation models, supported by snapshot simulations and data assimilation products. Additionally, we find no consistent trend in the internal variability of the overall AMOC, as the amplitude of decadal variations does not change noticeably between 6 ka to present in any of the simulations. Neither did this research show any consistent support for zonal mean streamfunction trends at particular latitudes or depths. This suggests that AMOC changes are unlikely to contribute to long-term (multi-millennial) global trends since the mid-Holocene (Kaufman & Broadman, 2023). We emphasize that this does not rule out AMOC playing an important role in ongoing and future climate changes (Fox-Kemper et al., 2021; Weijer et al., 2020).

Figure 4. Comparison of Atlantic Meridional Overturning Circulation (AMOC) simulations with reconstructions. (a) Ensemble mean of the nine transient simulations' maximum AMOC at 30°N, after each simulation has been standardized by conversion to a z-score over the period 6–0 ka BP. (b) The AMOC reconstruction identified in the reanalysis of Osman et al. (2021). This reanalysis combines marine geochemical data with climate model experiment using proxy system models and data assimilation. Dark and lighter shading on the timeseries indicate $\pm 1\sigma$ and 95% confidence intervals, respectively. (c) AMOC variations reconstructed by Ritz et al. (2013) using data assimilation with priors based on either LOVECLIM or Bern3D simulations. Gray dots are Pa/Th proxy data from Lippold et al. (2019), on the right axis. (d) AMOC variations resulting from applying an annualized SST index (after Caesar et al. (2018)) to the surface air temperature anomalies reconstructed by Erb et al. (2022) using data assimilation of the temperature 12k database (Kaufman et al., 2020).

Data Availability Statement

The data from the transient runs that used for analyzing the AMOC evolution throughout the Holocene in this study are available at Github repository (https://github.com/ZhiyiJiang/Transient-Holocene-AMOC/tree/v3.2) and are permanently archived at Zenodo (https://doi.org/10.5281/zenodo.7799682).

References

Aguiar, W., Meissner, K. J., Montenegro, A., Prado, L., Wainer, I., Carlson, A. E., & Mata, M. M. (2021). Magnitude of the 8.2 ka event freshwater forcing based on stable isotope modelling and comparison to future Greenland melting. *Scientific Reports*, *11*(1), 1–10. https://doi.org/10.1038/s41598-021-84709-5

Argus, D. F., Peltier, W., Drummond, R., & Moore, A. W. (2014). The Antarctica component of postglacial rebound model ICE-6G_C (VM5a) based on GPS positioning, exposure age dating of ice thicknesses, and relative sea level histories. *Geophysical Journal International*, *198*(1), 537–563. https://doi.org/10.1093/gji/ggu140

Ayache, M., Swingedouw, D., Mary, Y., Eynaud, F., & Colin, C. (2018). Multi-centennial variability of the AMOC over the Holocene: A new reconstruction based on multiple proxy-derived SST records. *Global and Planetary Change*, *170*, 172–189. https://doi.org/10.1016/j.gloplacha.2018.08.016

Bader, J., Jungclaus, J., Krivova, N., Lorenz, S., Maycock, A., Raddatz, T., et al. (2020). Global temperature modes shed light on the Holocene temperature conundrum. *Nature Communications*, *11*(1), 1–8. https://doi.org/10.1038/s41467-020-18478-6

Barber, D. C., Dyke, A., Hillaire-Marcel, C., Jennings, A. E., Andrews, J. T., Kerwin, M. W., et al. (1999). Forcing of the cold event of 8,200 years ago by catastrophic drainage of Laurentide lakes. *Nature*, *400*(6742), 344–348. https://doi.org/10.1038/22504

Braconnot, P., Zhu, D., Marti, O., & Servonnat, J. (2019). Strengths and challenges for transient mid-to late Holocene simulations with dynamical vegetation. *Climate of the Past*, *15*(3), 997–1024. https://doi.org/10.5194/cp-15-997-2019

Brierley, C. M., Zhao, A., Harrison, S. P., Braconnot, P., Williams, C. J., Thornalley, D. J., et al. (2020). Large-scale features and evaluation of the PMIP4-CMIP6 mid Holocene simulations. *Climate of the Past*, *16*(5), 1847–1872. https://doi.org/10.5194/cp-16-1847-2020

Caesar, L., McCarthy, G. D., Thornalley, D., Cahill, N., & Rahmstorf, S. (2021). Current Atlantic meridional overturning circulation weakest in last millennium. *Nature Geoscience*, *14*(3), 118–120. https://doi.org/10.1038/s41561-021-00699-z

Caesar, L., Rahmstorf, S., Robinson, A., Feulner, G., & Saba, V. (2018). Observed fingerprint of a weakening Atlantic Ocean overturning circulation. *Nature*, *556*(7700), 191–196. https://doi.org/10.1038/s41586-018-0006-5

Cherchi, A. (2019). Connecting AMOC changes. *Nature Climate Change*, *9*(10), 729–730. https://doi.org/10.1038/s41558-019-0590-x

Crosta, X., Crespin, J., Swingedouw, D., Marti, O., Masson-Delmotte, V., Etourneau, J., et al. (2018). Ocean as the main driver of Antarctic ice sheet retreat during the Holocene. *Global and Planetary Change*, *166*, 62–74. https://doi.org/10.1016/j.gloplacha.2018.04.007

Dallmeyer, A., Claussen, M., Lorenz, S. J., Sigl, M., Toohey, M., & Herzschuh, U. (2021). Holocene vegetation transitions and their climatic drivers in MPI-ESM1.2. *Climate of the Past*, *17*(6), 2481–2513. https://doi.org/10.5194/cp-17-2481-2021

Denton, G. H., & Broecker, W. S. (2008). Wobbly ocean conveyor circulation during the Holocene? *Quaternary Science Reviews*, *27*(21–22), 1939–1950. https://doi.org/10.1016/j.quascirev.2008.08.008

Erb, M. P., McKay, N. P., Steiger, N., Dee, S., Hancock, C., Ivanovic, R. F., et al. (2022). Reconstructing Holocene temperatures in time and space using paleoclimate data assimilation. *EGUsphere*, *18*(12), 1–48. https://doi.org/10.5194/cp-18-2599-2022

Fox-Kemper, B., Hewitt, H. T., Xiao, C., Aðalgeirsdóttir, G., Drijfhout, S., Edwards, T. L., et al. (2021). Ocean, cryosphere and sea level change. In V. Masson-Delmotte, P. Zhai, A. Pirani, S. L. Connors, C. Péan, S. Berger, et al. (Eds.), *Climate change 2021: The physical science basis. Contribution of working group 1 to the sixth assessment report of the intergovernmental panel on climate change (chap. 9)*. Cambridge University Press. https://doi.org/10.1017/9781009157896.011

Gulev, S., Thorne, P., Ahn, J., Dentener, F., Domingues, C., Gerland, S., et al. (2021). Changing state of the climate system. In V. Masson-Delmotte, P. Zhai, A. Pirani, S. L. Connors, C. Péan, S. Berger, et al. (Eds.), *Climate change 2021: The physical science basis. Contribution of working group 1 to the sixth assessment report of the intergovernmental panel on climate change (chap. 2)*. Cambridge University Press. https://doi.org/10.1017/9781009157896.004

He, F. (2011). Simulating transient climate evolution of the last deglaciation with CCSM3 (Vol. 72, No. (10)).

He, F., & Clark, P. U. (2022). Freshwater forcing of the Atlantic Ocean overturning circulation revisited. *Nature Climate Change*, *12*(5), 449–454. https://doi.org/10.1038/s41558-022-01328-2

Hoffmann, S. S., McManus, J. F., & Swank, E. (2018). Evidence for stable Holocene basin-scale overturning circulation despite variable currents along the deep western boundary of the North Atlantic Ocean. *Geophysical Research Letters*, *45*(24), 13427–13436. https://doi.org/10.1029/2018GL080187

Hopcroft, P. O., & Valdes, P. J. (2021). Paleoclimate-conditioning reveals a North Africa land–atmosphere tipping point. *Proceedings of the National Academy of Sciences of the United States of America*, *118*(45), e2108783118. https://doi.org/10.1073/pnas.2108783118

Hurtt, G. C., Chini, L. P., Frolking, S., Betts, R., Feddema, J., Fischer, G., et al. (2011). Harmonization of land-use scenarios for the period 1500–2100: 600 years of global gridded annual land-use transitions, wood harvest, and resulting secondary lands. *Climatic Change*, *109*(1), 117–161. https://doi.org/10.1007/s10584-011-0153-2

Ivanovic, R. F., Valdes, P. J., Flecker, R., Gregoire, L. J., & Gutjahr, M. (2013). The parameterisation of Mediterranean–Atlantic water exchange in the Hadley Centre model HadCM3, and its effect on modelled North Atlantic climate. *Ocean Modelling*, *62*, 11–16. https://doi.org/10.1016/j.ocemod.2012.11.002

Ivanovic, R. F., Valdes, P. J., Flecker, R., & Gutjahr, M. (2014). Modelling global-scale climate impacts of the late Miocene Messinian salinity crisis. *Climate of the Past*, *10*(2), 607–622. https://doi.org/10.5194/cp-10-607-2014

Jackson, L. C., Roberts, M. J., Hewitt, H. T., Iovino, D., Koenigk, T., Meccia, V. L., et al. (2020). Impact of ocean resolution and mean state on the rate of AMOC weakening. *Climate Dynamics*, *55*(7–8), 1711–1732. https://doi.org/10.1007/s00382-020-05345-9

Jalali, B., Sicre, M.-A., Azuara, J., Pellichero, V., & Combourieu-Nebout, N. (2019). Influence of the North Atlantic subpolar gyre circulation on the 4.2 ka BP event. *Climate of the Past*, *15*(2), 701–711. https://doi.org/10.5194/cp-15-701-2019

Jiang, Z., Brierley, C., Thornalley, D., & Sax, S. (2023). No changes in overall AMOC strength in interglacial PMIP4 time slices. *Climate of the Past*, *19*(1), 107–121. https://doi.org/10.5194/cp-19-107-2023

Kageyama, M., Braconnot, P., Harrison, S. P., Haywood, A. M., Jungclaus, J. H., Otto-Bliesner, B. L., et al. (2018). The PMIP4 contribution to CMIP6–Part 1: Overview and over-arching analysis plan. *Geoscientific Model Development*, *11*(3), 1033–1057. https://doi.org/10.5194/gmd-11-1033-2018

Kaufman, D. S., & Broadman, E. (2023). Revisiting the Holocene global temperature conundrum. *Nature*, *614*(7948), 425–435. https://doi.org/10.1038/s41586-021-03984-4

Kaufman, D. S., McKay, N., Routson, C., Erb, M., Davis, B., Heiri, O., et al. (2020). A global database of Holocene paleotemperature records. *Scientific Data*, *7*(1), 1–34. https://doi.org/10.1038/s41597-020-0445-3

Keigwin, L., & Boyle, E. (2000). Detecting Holocene changes in thermohaline circulation. *Proceedings of the National Academy of Sciences of the United States of America*, *97*(4), 1343–1346. https://doi.org/10.1073/pnas.97.4.1343

Kobashi, T., Menviel, L., Jeltsch-Thömmes, A., Vinther, B. M., Box, J. E., Muscheler, R., et al. (2017). Volcanic influence on centennial to millennial Holocene Greenland temperature change. *Scientific Reports*, *7*(1), 1–10. https://doi.org/10.1038/s41598-017-01451-7

Lawrence, D. M., Hurtt, G. C., Arneth, A., Brovkin, V., Calvin, K. V., Jones, A. D., et al. (2016). The land use model intercomparison project (LUMIP) contribution to CMIP6: Rationale and experimental design. *Geoscientific Model Development*, *9*(9), 2973–2998. https://doi.org/10.5194/gmd-9-2973-2016

Lippold, J., Pöppelmeier, F., Süfke, F., Gutjahr, M., Goepfert, T. J., Blaser, P., et al. (2019). Constraining the variability of the Atlantic meridional overturning circulation during the Holocene. *Geophysical Research Letters*, *46*(20), 11338–11346. https://doi.org/10.1029/2019gl084988

Lynch-Stieglitz, J., Curry, W. B., & Lund, D. C. (2009). Florida straits density structure and transport over the last 8000 years. *Paleoceanography*, *24*(3), PA3209. https://doi.org/10.1029/2008PA001717

Madec, G., Bourdallé-Badie, R., Bouttier, P. A., Bricaud, C., Bruciaferri, D., Calvert, D., et al. (2008). NEMO ocean engine, version 3.0. *Note du Pôle de modélisation de l'Institut Pierre-Simon Laplace*, *27*, 217. https://doi.org/10.5281/zenodo.3248739

Matero, I., Gregoire, L., Ivanovic, R., Tindall, J., & Haywood, A. (2017). The 8.2 ka cooling event caused by Laurentide ice saddle collapse. *Earth and Planetary Science Letters*, *473*, 205–214. https://doi.org/10.1016/j.epsl.2017.06.011

Mauritsen, T., Bader, J., Becker, T., Behrens, J., Bittner, M., Brokopf, R., et al. (2019). Developments in the MPI-M Earth System Model version 1.2 (MPI-ESM1.2) and its response to increasing CO_2. *Journal of Advances in Modeling Earth Systems*, *11*(4), 998–1038. https://doi.org/10.1029/2018MS001400

Ng, H. C., Robinson, L. F., McManus, J. F., Mohamed, K. J., Jacobel, A. W., Ivanovic, R. F., et al. (2018). Coherent deglacial changes in western Atlantic Ocean circulation. *Nature Communications*, *9*(1), 1–10. https://doi.org/10.1038/s41467-018-05312-3

Oppo, D. W., McManus, J. F., & Cullen, J. L. (2003). Palaeo-oceanography: Deepwater variability in the Holocene epoch. *Nature*, *422*(6929), 277–278. https://doi.org/10.1038/422277b

Osman, M. B., Tierney, J. E., Zhu, J., Tardif, R., Hakim, G. J., King, J., & Poulsen, C. J. (2021). Globally resolved surface temperatures since the last glacial maximum. *Nature*, *599*(7884), 239–244. https://doi.org/10.31223/x5s31z

Otto-Bliesner, B. L., Braconnot, P., Harrison, S. P., Lunt, D. J., Abe-Ouchi, A., Albani, S., et al. (2017). The PMIP4 contribution to CMIP6 - Part 2: Two interglacials, scientific objective and experimental design for Holocene and Last Interglacial simulations. *Geoscientific Model Development*, *10*(11), 3979–4003. https://doi.org/10.5194/gmd-10-3979-2017

Otto-Bliesner, B. L., Brady, E. C., Clauzet, G., Tomas, R., Levis, S., & Kothavala, Z. (2006). Last glacial maximum and Holocene climate in CCSM3. *Journal of Climate*, *19*(11), 2526–2544. https://doi.org/10.1175/JCLI3748.1

Peltier, W. R., Argus, D., & Drummond, R. (2015). Space geodesy constrains ice age terminal deglaciation: The global ICE-6G_C (VM5a) model. *Journal of Geophysical Research: Solid Earth*, *120*(1), 450–487. https://doi.org/10.1002/2014jb011176

Rahmstorf, S. (2006). Thermohaline ocean circulation. *Encyclopedia of Quaternary Sciences*, *5*.

Rahmstorf, S., Box, J. E., Feulner, G., Mann, M. E., Robinson, A., Rutherford, S., & Schaffernicht, E. J. (2015). Exceptional twentieth-century slowdown in Atlantic Ocean overturning circulation. *Nature Climate Change*, *5*(5), 475–480. https://doi.org/10.1038/nclimate2554

Rennsen, H., Goosse, H., & Fichefet, T. (2005). Contrasting trends in North Atlantic deep-water formation in the Labrador Sea and Nordic Seas during the Holocene. *Geophysical Research Letters*, *32*(8), L08711. https://doi.org/10.1029/2005gl022462

Ritz, S. P., Stocker, T. F., Grimalt, J. O., Menviel, L., & Timmermann, A. (2013). Estimated strength of the Atlantic overturning circulation during the last deglaciation. *Nature Geoscience*, *6*(3), 208–212. https://doi.org/10.1038/ngeo1723

Roeckner, E., Bäuml, G., Bonaventura, L., Brokopf, R., Esch, M., Giorgetta, M., et al. (2003). The atmospheric general circulation model ECHAM 5. PART I: Model description. Max-Planck-Institut für Meteorologie internal report (Vol. *349*, p. 144).

Segschneider, J., Schneider, B., & Khon, V. (2018). Climate and marine biogeochemistry during the Holocene from transient model simulations. *Biogeosciences*, *15*(10), 3243–3266. https://doi.org/10.5194/bg-15-3243-2018

Shi, X., & Lohmann, G. (2016). Simulated response of the mid-Holocene Atlantic Ocean overturning circulation in ECHAM6-FESOM/MPIOM. *Journal of Geophysical Research: Oceans*, *121*(8), 6444–6469. https://doi.org/10.1002/2015jc011584

Shi, X., Lohmann, G., Sidorenko, D., & Yang, H. (2020). Early-Holocene simulations using different forcings and resolutions in AWI-ESM. *The Holocene*, *30*(7), 996–1015. https://doi.org/10.1177/0959683620908634

Shi, X., Werner, M., Krug, C., Brierley, C. M., Zhao, A., Igbinosa, E., et al. (2022). Calendar effects on surface air temperature and precipitation based on model-ensemble equilibrium and transient simulations from PMIP4 and PACMEDY. *Climate of the Past*, *18*(5), 1047–1070. https://doi.org/10.5194/cp-18-1047-2022

Sidorenko, D., Goessling, H. F., Koldunov, N., Scholz, P., Danilov, S., Barbi, D., et al. (2019). Evaluation of FESOM2.0 coupled to ECHAM6. 3: Preindustrial and HighResMIP simulations. *Journal of Advances in Modeling Earth Systems*, *11*(11), 3794–3815. https://doi.org/10.1029/2019MS001696

Smeed, D. A., Josey, S., Beaulieu, C., Johns, W., Moat, B. I., Frajka-Williams, E., et al. (2018). The North Atlantic Ocean is in a state of reduced overturning. *Geophysical Research Letters*, *45*(3), 1527–1533. https://doi.org/10.1002/2017GL076350

Smith, B. D., & Zeder, M. A. (2013). The onset of the anthropocene. *Anthropocene*, *4*, 8–13. https://doi.org/10.1016/j.ancene.2013.05.001

Swingedouw, D., Colin, C., Eynaud, F., Ayache, M., & Zaragosi, S. (2019). Impact of freshwater release in the Mediterranean Sea on the North Atlantic climate. *Climate Dynamics*, *53*(7), 3893–3915. https://doi.org/10.1007/s00382-019-04758-5

Thornalley, D. J., Oppo, D. W., Ortega, P., Robson, J. I., Brierley, C. M., Davis, R., et al. (2018). Anomalously weak Labrador Sea convection and Atlantic overturning during the past 150 years. *Nature*, *556*(7700), 227–230. https://doi.org/10.1038/s41586-018-0007-4

Tian, Z., Jiang, D., Zhang, R., & Su, B. (2022). Transient climate simulations of the Holocene (version 1)–experimental design and boundary conditions. *Geoscientific Model Development*, *15*(11), 4469–4487. https://doi.org/10.5194/gmd-15-4469-2022

Valley, S. G., Lynch-Stieglitz, J., Marchitto, T. M., & Oppo, D. W. (2022). Seawater cadmium in the Florida Straits over the Holocene and implications for upper AMOC variability. *Paleoceanography and Paleoclimatology*, *37*(5), e2021PA004379. https://doi.org/10.1029/2021pa004379

Vieira, L. E. A., Solanki, S. K., Krivova, N. A., & Usoskin, I. (2011). Evolution of the solar irradiance during the Holocene. *Astronomy & Astrophysics*, *531*, A6. https://doi.org/10.1051/0004-6361/201015843

Weijer, W., Cheng, W., Garuba, O. A., Hu, A., & Nadiga, B. T. (2020). CMIP6 models predict significant 21st century decline of the Atlantic Ocean overturning circulation. *Geophysical Research Letters*, *47*(12), e2019GL086075. https://doi.org/10.1029/2019GL086075

Zhang, Q., Berntell, E., Axelsson, J., Chen, J., Han, Z., De Nooijer, W., et al. (2021). Simulating the mid-Holocene, last interglacial and mid-Pliocene climate with EC-Earth3-LR. *Geoscientific Model Development*, *14*(2), 1147–1169. https://doi.org/10.5194/gmd-14-1147-2021

References From the Supporting Information

Augustin, L., Barbante, C., Barnes, P. R., Barnola, J. M., Bigler, M., Castellano, E., et al. (2004). Eight glacial cycles from an Antarctic ice core. *Nature*, *429*(6992), 623–628. https://doi.org/10.1038/nature02599

Bereiter, B., Eggleston, S., Schmitt, J., Nehrbass-Ahles, C., Stocker, T. F., Fischer, H., et al. (2015). Revision of the EPICA Dome C CO_2 record from 800 to 600 kyr before present. *Geophysical Research Letters*, *42*(2), 542–549. https://doi.org/10.1002/2014gl061957

Berger, A. (1978). Long-term variations of daily insolation and quaternary climatic changes. *Journal of the Atmospheric Sciences*, *35*(12), 2362–2367. https://doi.org/10.1175/1520-0469(1978)035⟨2362:ltvodi⟩2.0.co;2

Berger, A., & Loutre, M. F. (1991). Insolation values for the climate of the last 10 million years. *Quaternary Science Reviews*, *10*(4), 297–317. https://doi.org/10.1016/0277-3791(91)90033-Q

Brovkin, V., Lorenz, S., Raddatz, T., Ilyina, T., Stemmler, I., Toohey, M., & Claussen, M. (2019). What was the source of the atmospheric CO_2 increase during the Holocene? *Biogeosciences*, *16*(13), 2543–2555. https://doi.org/10.5194/bg-16-2543-2019

Clark, P. U., & Mix, A. C. (2002). Ice sheets and sea level of the last glacial maximum. *Quaternary Science Reviews*, *21*(1–3), 1–7. https://doi.org/10.1016/S0277-3791(01)00118-4

Collins, W. D., Bitz, C. M., Blackmon, M. L., Bonan, G. B., Bretherton, C. S., Carton, J. A., et al. (2006). The community climate system model version 3 (CCSM3). *Journal of Climate*, *19*(11), 2122–2143. https://doi.org/10.1175/JCLI3761.1

Cox, P. M. (2001). Description of the 'TRIFFID' dynamic global vegetation model. *Tech. Note*, *24*.

Döscher, R., Acosta, M., Alessandri, A., Anthoni, P., Arsouze, T., Bergman, T., et al. (2022). The EC-Earth3 Earth system model for the coupled model intercomparison project 6. *Geoscientific Model Development*, *15*(7), 2973–3020. https://doi.org/10.5194/gmd-15-2973-2022

Jin, L., Schneider, B., Park, W., Latif, M., Khon, V., & Zhang, X. (2014). The spatial–temporal patterns of Asian summer monsoon precipitation in response to Holocene insolation change: A model-data synthesis. *Quaternary Science Reviews*, *85*, 47–62. https://doi.org/10.1016/j.quascirev.2013.11.004

Joos, F., & Spahni, R. (2008). Rates of change in natural and anthropogenic radiative forcing over the past 20,000 years. *Proceedings of the National Academy of Sciences of the United States of America*, *105*(5), 1425–1430. https://doi.org/10.1073/pnas.0707386105

Khon, V., Park, W., Latif, M., Mokhov, I., & Schneider, B. (2010). Response of the hydrological cycle to orbital and greenhouse gas forcing. *Geophysical Research Letters*, *37*(19), L19705. https://doi.org/10.1029/2010gl044377

Khon, V. C., Schneider, B., Latif, M., Park, W., & Wengel, C. (2018). Evolution of eastern equatorial Pacific seasonal and interannual variability in response to orbital forcing during the Holocene and Eemian from model simulations. *Geophysical Research Letters*, *45*(18), 9843–9851. https://doi.org/10.1029/2018gl079337

Köhler, P., Nehrbass-Ahles, C., Schmitt, J., Stocker, T. F., & Fischer, H. (2017). A 156 kyr smoothed history of the atmospheric greenhouse gases CO_2, CH_4, and N_2O and their radiative forcing. *Earth System Science Data*, *9*(1), 363–387. https://doi.org/10.5194/essd-9-363-2017

Liu, Z., Otto-Bliesner, B., He, F., Brady, E., Tomas, R., Clark, P., et al. (2009). Transient simulation of last deglaciation with a new mechanism for Bølling-Allerød warming. *Science*, *325*(5938), 310–314. https://doi.org/10.1126/science.1171041

Loulergue, L., Schilt, A., Spahni, R., Masson-Delmotte, V., Blunier, T., Lemieux, B., et al. (2008). Orbital and millennial-scale features of atmospheric CH_4 over the past 800,000 years. *Nature*, *453*(7193), 383–386. https://doi.org/10.1038/nature06950

Park, W., Keenlyside, N., Latif, M., Ströh, A., Redler, R., Roeckner, E., & Madec, G. (2009). Tropical Pacific climate and its response to global warming in the KIEL climate model. *Journal of Climate*, *22*(1), 71–92. https://doi.org/10.1175/2008jcli2261.1

Peltier, W. R. (2004). Global glacial isostasy and the surface of the ice-age Earth: The ICE-5G (VM2) model and grace. *Annual Review of Earth and Planetary Sciences*, *32*(1), 111–149. https://doi.org/10.1146/annurev.earth.32.082503.144359

Rousset, C., Vancoppenolle, M., Madec, G., Fichefet, T., Flavoni, S., Barthélemy, A., et al. (2015). The Louvain-La-Neuve sea ice model LIM3.6: Global and regional capabilities. *Geoscientific Model Development*, *8*(10), 2991–3005. https://doi.org/10.5194/gmd-8-2991-2015

Salau, O., Schneider, B., Park, W., Khon, V., & Latif, M. (2012). Modeling the ENSO impact of orbitally induced mean state climate changes. *Journal of Geophysical Research*, *117*(C5), C05043. https://doi.org/10.1029/2011jc007742

Schilt, A., Baumgartner, M., Schwander, J., Buiron, D., Capron, E., Chappellaz, J., et al. (2010). Atmospheric nitrous oxide during the last 140,000 years. *Earth and Planetary Science Letters*, *300*(1–2), 33–43. https://doi.org/10.1016/j.epsl.2010.09.027

Smith, B., Wårlind, D., Arneth, A., Hickler, T., Leadley, P., Siltberg, J., & Zaehle, S. (2014). Implications of incorporating N cycling and N limitations on primary production in an individual-based dynamic vegetation model. *Biogeosciences*, *11*(7), 2027–2054. https://doi.org/10.5194/bg-11-2027-2014

Toohey, M., Stevens, B., Schmidt, H., & Timmreck, C. (2016). Easy volcanic aerosol (EVA v1.0): An idealized forcing generator for climate simulations. *Geoscientific Model Development*, *9*(11), 4049–4070. https://doi.org/10.5194/gmd-9-4049-2016

Valdes, P. J., Armstrong, E., Badger, M. P., Bradshaw, C. D., Bragg, F., Crucifix, M., et al. (2017). The BRIDGE HadCM3 family of climate models: HadCM3@ bristol v1.0. *Geoscientific Model Development*, *10*(10), 3715–3743. https://doi.org/10.5194/gmd-2017-16-rc1

Veres, D., Bazin, L., Landais, A., Toyé Mahamadou Kele, H., Lemieux-Dudon, B., Parrenin, F., et al. (2013). The Antarctic ice core chronology (AICC2012): An optimized multi-parameter and multi-site dating approach for the last 120 thousand years. *Climate of the Past*, *9*(4), 1733–1748. https://doi.org/10.5194/cp-9-1733-2013